Electron flow driven instability in finite beta plasmas

I. Pusztai[1,2], P. J. Catto[1], F. I. Parra[1], M. Barnes[1]

[1] *Plasma Science and Fusion Center, Massachusetts Inst. of Technology, Cambridge MA, USA*

[2] *Applied Physics, Chalmers University of Technology and Euratom-VR Association, Göteborg, Sweden*

Ohmic current as a drive for instabilities in tokamaks can be modeled in the *low-flow* version of GS2 [1]. We identify kink modes in GS2 and make comparisons to analytical results.

Introduction The radial gradient of electric current represents a source of free energy in fusion plasmas which can drive or modify instabilities. Using the new version of the gyrokinetic code GS2 developed for momentum transport studies [1], we are able to model the effect of the induced parallel electric field on the electron distribution, thus study the impact of a current.

Dispersion relation of high-m kink modes First we present the electromagnetic dispersion relation of high-m kink modes in a simplified tokamak geometry. We consider a large aspect ratio $r/R \ll 1$, circular cross-section, low-β, toroidally symmetric equilibrium; and assume a flute-like mode structure $e^{-i\omega t+im\theta-in\zeta}$ for the perturbed quantities. Magnetic drifts, magnetic shear effects and compressional magnetic perturbations are neglected. The induced electron current is represented as a parallel electron flow speed $-u$. The non-fluctuating part of the electron distribution is written as $f_{0e} = f_{*e}(\psi_*, E) + f_s(\mathbf{R}, E, \mu)$, where $E = v^2/2 + (e_a/m_a)\phi_0$, $\psi_* = \psi - (m_a c/e_a)R\hat{\zeta}\cdot\mathbf{v}$, $\mathbf{R}$ is the guiding center position, $f_s = -m_e v_\parallel u f_{Me}/T_e$. $f_{*a} = \eta_{*a}\left(m_a/2\pi T_{*a}\right)^{3/2}\exp\left(-m_a E/T_{*a}\right)$, where $T_{*a} = T_a(\psi = \psi_*)$ with T_a the species temperature, and the pseudo-density is $\eta_{*a} = n_{*a}\exp[e_a\phi_{0*}/T_{*a}]$ with $\phi_{0*} = \phi_0(\psi = \psi_*)$ and $n_{*a} = n_a(\psi = \psi_*)$. We consider $\phi_0 = 0$. $f_{Ma} = f_{*a}(\psi_* \to \psi)$. The linearized kinetic equation for the fluctuating part of the electron distribution f_{1e} can be written as $d_t f_{1e} = -(e_e/m_e)\left(\mathbf{E}_1 + \mathbf{v}\times\mathbf{B}_1/c\right)\cdot \nabla_v f_{0e}$, with d_t the unperturbed Vlasov operator, and the perturbed fields $\mathbf{E}_1 = -\nabla\phi_1 - \partial_t\mathbf{A}_1/c$, $\mathbf{B}_1 = \nabla\times\mathbf{A}_1$.

Then following a procedure similar to that in [2] we can derive the gyro-kinetic equation assuming $u \gg \rho_{*e\theta}v_e$. In the process, finite orbit width effects are neglected where it is appropriate, and for electrons we also neglect finite Larmor radius corrections to obtain

$$(\partial_t + v_\parallel \mathbf{b}\cdot\nabla)g_e = (e_e/T_e)f_{Me}(1 - m_e v_\parallel u/T_e)(\partial_t\phi_1 - v_\parallel\partial_t A_\parallel/c)$$
$$-cf_{Me}(\partial_\zeta\phi_1 - v_\parallel\partial_\zeta A_\parallel/c)(F_{1e} - m_e v_\parallel u F_{2e}/T_e) + e_e u f_{Me}E_\parallel/T_e, \quad (1)$$

where $g_e = f_{1e} + f_{Me}(1 - m_e v_\parallel u/T_e) e_e \phi_1/T_e$, with $F_{1a} = (\ln n_a)' + [m_a v^2/(2T_a) - 3/2](\ln T_a)'$ and $F_{2e} = (\ln j_0)' + [m_e v^2/(2T_e) - 5/2](\ln T_e)'$. The ψ-derivative is denoted by $'$, $j_0 = -e n_e u$ is the current density and $E_\parallel = \mathbf{b}\cdot\mathbf{E}_1$. Similarly, for ions we find

$$(\partial_t + v_\parallel \mathbf{b}\cdot\nabla) g_i = (e_i/T_i) f_{Mi} (\partial_t \langle\phi_1\rangle - v_\parallel \partial_t \langle A_\parallel\rangle/c) - c f_{Mi} (\partial_\zeta \langle\phi_1\rangle - v_\parallel \partial_\zeta \langle A_\parallel\rangle/c) F_{1i}. \quad (2)$$

We use $\partial_t(\sum_a e_a \int d^3v g_a) + \mathbf{B}\cdot\nabla(\sum_a e_a \int d^3v v_\parallel g_a/B) = \sum_a e_a \int d^3v \mathrm{RHS}_a$, where RHS_a denotes the right hand sides of (1) and (2), to find

$$(e_e^2 n_e/T_e)(1+\tau)\partial_t\phi_1 + \mathbf{B}\cdot\nabla[j_\parallel/B - (e_e n_e u/B)(e_e\phi_1/T_e)] = (e_e^2 n_e/T_e)$$
$$\times\{[1+\tau(1-\alpha_i)]\partial_t\phi_1 + u\partial_t A_\parallel/c\} + e_i n_i c (\ln p_i)'\alpha_i \partial_\zeta\phi_1 - e_e u n_e \partial_\zeta A_\parallel (\ln j_0)' + e_e^2 n_e u E_\parallel/T_e, \quad (3)$$

where $j_\parallel$ is the perturbed parallel current, $\tau = (T_e/T_i)|e_i/e_e|$, and we kept only linear corrections in $\alpha_i = (k_\perp \rho_i)^2/2$. In terms of ω and $k_\parallel$, (3) simplifies to $i k_\parallel j_\parallel = i\omega\tau\alpha_i e_e^2 n_e \phi_1/T_e - i n e_i n_i c (\ln p_i)'\alpha_i\phi_1$
$+ i n e_e u n_e A_\parallel (\ln j_0)'$. We employ the perpendicular Ampère's law $k_\perp^2 A_\parallel = (4\pi/c) j_\parallel$, and assume $E_\parallel = 0 \Rightarrow \phi_1 = \omega A_\parallel/(k_\parallel c)$ to eliminate ϕ_1. With the definitions $\beta_i = 8\pi p_i/B^2$, $\omega_{*i}^p = (n c T_i/e_i)(\ln p_i)'$ and $\omega_{*e}^j = (n c T_e/e_e)(\ln j_0)'$ we obtain

$$\omega = \frac{\omega_{*i}^p}{2} \pm \left[\left(\frac{\omega_{*i}^p}{2}\right)^2 + \frac{(v_i k_\parallel)^2}{\beta_i} - \frac{2\omega_{*e}^j k_\parallel u}{\tau(k_\perp\rho_i)^2}\right]^{1/2}. \quad (4)$$

This result is consistent with Equation (15) of [3], derived in a shear-less slab geometry. The ω_{*e}^j term may dominate the expression in the bracket in (4), which corresponds to the appearance of a growing mode, the growth rate of which increases with decreasing $k_\perp$.

To study the effect of magnetic shear on the instability we may derive a dispersion relation in a sheared slab magnetic geometry where the unperturbed magnetic field is $\mathbf{B} = B(\hat{z} + \hat{y}x/L_s)$. The background plasma parameters vary in the $\hat{x}$-direction. The $\hat{x}$-component of the perturbed magnetic field has the form $B_x = \hat{B}(x) e^{-i\omega t + i k_y y}$, and $k_\parallel(x) = k_y x/L_s$. We introduce $X = k_y x$, to find the dispersion relation in the form of an eigenvalue problem

$$X\left(\partial_{XX}^2 - 1\right)\hat{B} - \lambda\left(\partial_{XX}^2 - 1\right)\left(\hat{B}/X\right) - \sigma\hat{B} = 0, \quad (5)$$

where $\lambda = \omega(\omega - \omega_{*i}^p) L_s^2 \beta_i/v_i^2 \approx \omega^2 L_s^2 \beta_i/v_i^2$ is the eigenvalue and $\sigma = -2 L_s \beta_i u \omega_{*e}^j/(\tau k_y^2 \rho_i^2 v_i^2)$ represents the drive. We require $\hat{B}(X \to \pm\infty) \to 0$. Since typically $\omega_{*i}^p \ll \omega$, we will refer to the modes with $\lambda < 0$ as unstable modes. For $|\sigma| = 2n$ with a non-zero integer n, the marginally stable ($\lambda = 0$) solutions of (5) are of the form $\hat{B}(X) = X e^{-X} {}_1F_1(1 + \sigma/2, 2, 2X) = X e^X P_\sigma(X)$

for $X \leq 0$ and $\hat{B}(X) = 0$ for $X > 0$. Here, ${}_1F_1$ denotes the Kummer confluent hypergeometric function, and P_σ is a polynomial with only positive coefficients. The derivative of the marginally stable solutions is discontinuous at $X = 0$, however it is resolved by a boundary layer at $+0$ for $|\sigma| = 2n + \delta$ with a small $\delta > 0$. The boundary layer connects the $X \leq 0$ solution to a solution $\propto e^{-X}[1 + 2Xe^{2X}\mathrm{Ei}(-2X)]$ for $X > 0$. When $|\sigma| \neq 2n$, no marginally stable ($\lambda = 0$) solution to (5) exists that would be consistent with both boundary conditions.

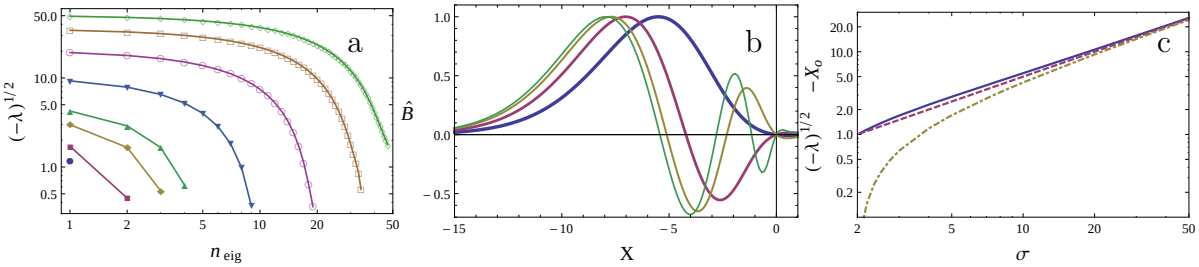

Figure 1: *Solutions of the eigenvalue problem (5). a:* $(-\lambda)^{1/2}$ *of unstable modes corresponding to* $\sigma = \{4, 5, 7.5, 10, 20, 40, 70, 100\}$*; the number of unstable modes* $\max(n_{\mathrm{eig}})$ *increases with* σ*. b:* $\hat{B}(X)$ *of the four unstable mode at* $\sigma = 10$*. c: Solid curve:* $-X_o$*, where* X_o *is the location of the maximum of* $|\hat{B}(X)|$ *for the most unstable mode for given* σ*. Dash-dotted curve:* $(-\lambda)^{1/2}$ *of the most unstable mode. Dashed curve:* $\sigma/2$*.*

The mode is stable for $|\sigma| < 2$, and a new unstable mode appears at every $|\sigma| = 2n$, as illustrated through the numerical solution of (5) in Fig. 1a, where the markers on a curve correspond to different eigenmodes for a fixed σ. For a given σ, eigenfunctions having smaller growth rates have more oscillatory radial mode structure, as shown in Fig. 1b. The location of the maximum of $\hat{B}$, denoted by X_o, moves away from the origin as $|\sigma|$ increases (and the corresponding $|k_\parallel|$ increases). The parallel wave number that maximizes the growth rate in shear-less geometry is $k_{\parallel o} = (u\beta_i\omega^j_{*e})/[v_i^2(k_y\rho_i)^2\tau]$; corresponding to $X = -\sigma/2$ in sheared geometry. The maximum growth rate is $\gamma_o = (u\sqrt{\beta_i}\omega_{*e})/[v_i(k_y\rho_i)^2\tau]$, which corresponds to $\sqrt{-\lambda} = \sigma/2$. In a sheared slab X_o and $\sqrt{-\lambda}$ approaches these values for increasing $|\sigma|$ as seen in Fig. 1c.

Using $1/L_s = s/qR$, $k_y = nq/r$ and $n = m/q$, it can be shown that the stability criterion $|\sigma| < 2$ is equivalent with that of the kink instability, Eq. (2.29) in [4]: $4\pi r|\partial_r j_0|/(cB_\theta) < 2m|q'/q|$.

Comparison of sheared slab and GS2 simulations We compare GS2 simulations in toroidal geometry to the predictions of the sheared slab model (SSM). In GS2 magnetic drifts and other effects of the toroidal geometry are accounted for in contrast to the SSM, and the complete lowest order gyrokinetic-Maxwell system of equations is solved. In toroidal geometry a is the minor radius, while it is only a unit of length in the SSM. The comparison in the form of

different parameter scalings around a set of baseline parameters is shown Fig. 2a-e. Considering the strong simplifying assumptions leading to the sheared slab dispersion relation (5) we find a reasonably good agreement between GS2 and the SSM in terms of mode frequencies and growth rates; the agreement improves for stronger instability drive (such as higher β_i, u, $(k_y\rho_i)^{-1}$). The radial eigenfunction in the SSM, $\hat{B}(X)$, is related to the ballooning eigenfunction $B_\psi(\theta)$ by a Fourier transformation $\mathcal{F}$, as $\hat{B}(X) \propto \mathcal{F}^{-1}[B_\psi(-\theta/s)]$. In Fig. 2f we compare the normalized amplitude of $\hat{B}(X)$ as obtained from the SSM (dashed) and calculated from the GS2 results for $A_\parallel(\theta)$, showing a convincing agreement.

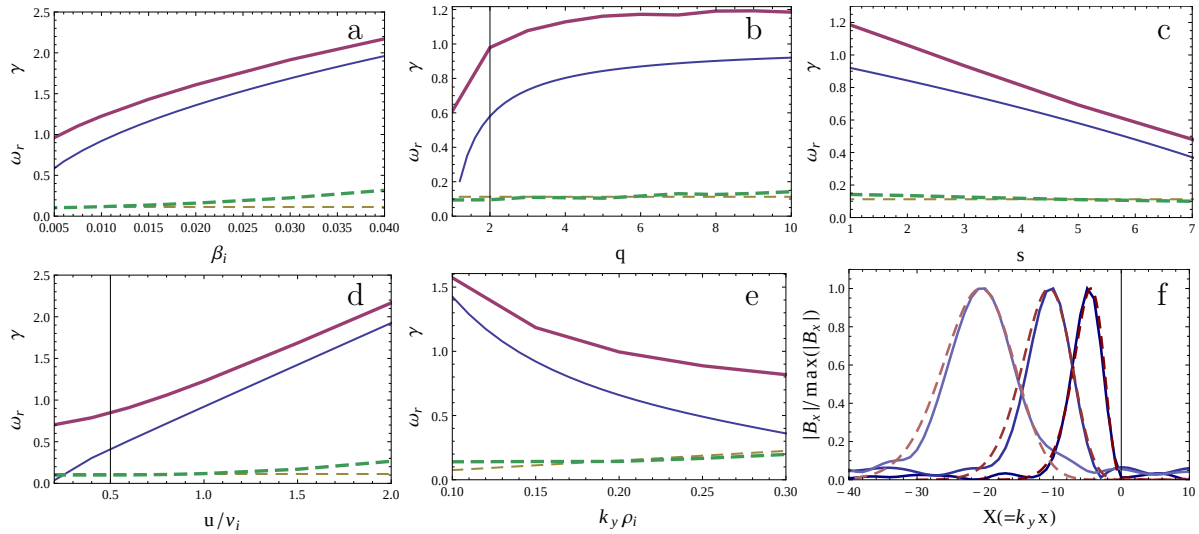

Figure 2: *real frequencies $\omega_r[v_i/a]$ (dashed lines), and growth rates $\gamma[v_i/a]$ (solid lines) of the highest-γ kink mode in the sheared slab model (thin lines) and in GS2 (thick lines). a-e: scalings with β_i, safety factor q, magnetic shear s, electron flow speed u, $k_y\rho_i$, respectively. f: Radial eigenfunctions in sheared slab (dashed) and in GS2 (solid) for $\beta_i = \{0.004, 0.01, 0.02\}$. Baseline parameters: $u/v_i = 1$, $\beta_i = 0.01$, $a/L_n = 3$, $a/L_{Ti} = a/L_{Te} = a/L_u = 0$, $k_y\rho_i = 0.15$, $a/R = 0.1$, $r/a = 0.5$, $s = 1$, $q = 10$, $\nu_{ei} = 0$*

Conclusions The effect of current gradient as a drive for microinstabilities is modeled using the low-flow version of GS2. We compare kink modes in GS2 to simplified analytical theory and find a reassuring agreement. GS2 may be used to study current gradient effects on instabilities.

References

[2] Barnes et al 2013 accepted for publication in *Phys. Rev. Lett.*, arXiv: 1304.3633.
[2] Catto P J 1978 *Plasma Phys.* **20** 719.
[3] Sperling J L and Bhadra D K 1979 *Plasma Phys.* **21** 225.
[4] Kadomtsev B B and Pogutse O P 1970 *Rev. Plasma Phys.* Vol**5** 249, ed. Leontovich M A.

Acknowledgments This work was funded by the European Communities under Association Contract between EURATOM and Vetenskapsrådet (VR), and by the US Department of Energy grant at DE-FG02-91ER-54109 at MIT. The first author is grateful for the financial support of VR.